J. Korean Math. Soc. **56** (2019), No. 3, pp. 805–823
https://doi.org/10.4134/JKMS.j180433
pISSN: 0304-9914 / eISSN: 2234-3008

C^1 HERMITE INTERPOLATION WITH MPH CURVES USING PH-MPH TRANSITIVE MAPPINGS

Gwangil Kim, Jae Hoon Kong, and Hyun Chol Lee

Abstract. We introduce polynomial PH-MPH transitive mappings which transform planar PH curves to MPH curves in $\mathbb{R}^{2,1}$, and prove that parameterizations of Enneper surfaces of the 1st and the 2nd kind and conjugates of Enneper surfaces of the 2nd kind are PH-MPH transitive. We show how to solve C^1 Hermite interpolation problems in $\mathbb{R}^{2,1}$, for an admissible C^1 Hermite data-set, by using the parametrization of Enneper surfaces of the 1st kind. We also show that we can obtain interpolants for at least some inadmissible data-sets by using MPH biarcs on Enneper surfaces of the 1st kind.

1. Introduction

Pythagorean-hodograph (PH) curves in $\mathbb{R}^2$ were originally introduced by Farouki and Sakkalis [9] as polynomial curves with polynomial speed functions. The properties of their speed functions provide computational advantages in handling offsets for NC machining.

PH curves have been the subject of a lot of research [4, 20]. Several different representations have been proposed for PH curves: a complex-variable model [9], a model based on the characterization of the complex roots of the hodograph of the curve [15], and a unified approach using Clifford algebra [3]. The original planar PH curves have been extended to spatial and rational curves [5, 10]; and methods of characterizing PH curves have become more sophisticated, and now encompass several more applications [20]. PH curves have also been extended to non-Euclidean space: in particular Minkowski PH (MPH) curves [23] have been used to solve problems related to Medial axis transformations [2, 21, 25]. These developments have included a lot of progress [1, 8, 11, 18, 19, 21, 24] in solving interpolation problems with PH/MPH

Received June 29, 2018; Revised July 21, 2018; Accepted August 2, 2018.
2010 *Mathematics Subject Classification.* Primary 65D17, 65D18, 68U05.
Key words and phrases. Minkowski Pythagorean-hodograph curve, PH-MPH transitive mapping, MPH-preserving mapping, C^1 Hermite data-set, C^1 Hermite interpolation.
This research was supported by Basic Science Research Program through the National Research Foundation of Korea(NRF) funded by the Ministry of Science, ICT and Future Planning(NRF-2017R1E1A1A03070952).

curves [5, 6, 12], including techniques such as speed re-parametrization [15], boundary data modification [16] and PH/MPH-preserving mappings [13,17,22].

In this paper, we introduce PH-MPH transitive mappings, which transform PH curves in $\mathbb{R}^2$ to MPH curves in $\mathbb{R}^{2,1}$, and we show that the mappings can be used to solve interpolation problems with MPH curves in $\mathbb{R}^{2,1}$, by reducing them to interpolation problems that can be solved using PH curves in $\mathbb{R}^2$. PH and MPH curves are geometrically associated [19], in their respective functions as boundary curves of planar domains and MATs, they have similar formulations, and their hodographs satisfy the same Pythagorean property: the difference between them is the metric of the space in which each is defined. We will demonstrate a new association between them: a functional association through PH-MPH transitive mappings. The algebraic similarity of PH and MPH curves is illustrated by their susceptibility to be handled in a unified way using Clifford algebra [3]. However, the use of this algebra to address interpolation problems with MPH curves directly can incur computational problems which do not arise when it is applied to PH curves. We will show that PH-MPH transitive mappings simplify the use of MPH curves to solve C^1 Hermite interpolation problems. Previous work based on Clifford algebra addressed C^1 Hermite interpolation in $\mathbb{R}^{2,1}$ using MPH quintics [18]. Subsequently in [19], this algebra was abandoned in favor of a unified Pythagorean hodograph approach, and it was shown that it is possible to solve G^1 Hermite interpolation problems in $\mathbb{R}^{2,1}$ with planar PH curves. We will show that it is possible to solve C^1 Hermite interpolation problems for admissible data-sets in $\mathbb{R}^{2,1}$ with planar PH quintics, by reducing them to interpolation problems in $\mathbb{R}^2$, using PH-MPH transitive mappings based on parameterizations of Enneper surfaces in $\mathbb{R}^{2,1}$.

The rest of this paper is organized as follows: In Section 2, we revisit the definitions of Pythagorean-hodograph (PH) and Minkowski Pythagorean-hodograph (MPH) curves, introduce PH-MPH transitive mappings and provide some examples. In Section 3, we show that parameterizations of the Enneper surfaces in $\mathbb{R}^{2,1}$ are PH-MPH transitive, and that two Enneper surfaces can be found to satisfy any admissible data-set in $\mathbb{R}^{2,1}$. We also show that these mappings can be used to reduce a C^1 Hermite interpolation problem involving such a data-set to a new C^1 Hermite interpolation problem in $\mathbb{R}^2$, and that there exist eight interpolants satisfying the original data-set, which lie on two Enneper surfaces as images, mapped by the parameterizations, of the planar PH quintic interpolants satisfying the reduced data-set in $\mathbb{R}^2$. We go on to consider inadmissible data-sets and, by means of an example, show that the junction-point method [15] using MPH biarcs might be a possible solution in this case. In Section 4, we summarize the results of this work and propose some themes for further study.

2. Preliminaries

For $n \in \mathbb{N}$, let $\mathbb{R}^{n+1}$ and $\mathbb{R}^{n,1}$ respectively be $(n+1)$-dimensional Euclidean and Minkowski space, and let $\mathbb{P}[t]$ be the set of polynomial functions with real coefficients. We will express a polynomial curve in $\mathbb{R}^{n+1}$ or $\mathbb{R}^{n,1}$ respectively as a mapping $\mathbf{r} : \mathbb{R} \to \mathbb{R}^{n+1}$ or $\mathbf{r} : \mathbb{R} \to \mathbb{R}^{n,1}$ from the space of real numbers $\mathbb{R}$ to $\mathbb{R}^{n+1}$ or $\mathbb{R}^{n,1}$. The component functions of $\mathbf{r}$, which are $x_1(t), x_2(t), \ldots, x_{n+1}(t)$, are members of $\mathbb{P}[t]$.

Definition 2.1. A polynomial curve $\mathbf{r}(t) = (x_1(t), x_2(t), \ldots, x_{n+1}(t))$ is said to be a *Pythagorean-hodograph* (*PH*) or a *Minkowski Pythagorean-hodograph* (*MPH*) curve if its hodograph $\mathbf{r}'(t) = (x_1'(t), \ldots, x_{n+1}'(t))$ satisfies the Pythagorean or the Minkowski Pythagorean condition respectively;

$$\|\mathbf{r}'(t)\|_{n+1}^2 = \sum_{i=1}^{n+1} x_i'(t)^2 = \sigma(t)^2 \left(\|\mathbf{r}'(t)\|_{n,1}^2 = \sum_{i=1}^{n} x_i'(t)^2 - x_{n+1}'(t)^2 = \sigma(t)^2 \right),$$

where $\| * \|_{n+1}$ ($\| * \|_{n,1}$) denotes the Euclidean or Minkowski norm of $\mathbb{R}^{n+1}$ or $\mathbb{R}^{n,1}$, and $\sigma(t) \in \mathbb{P}[t]$.

Definition 2.2. A polynomial mapping $\phi \colon \mathbb{R}^n \to \mathbb{R}^m$ or $\phi \colon \mathbb{R}^{n,1} \to \mathbb{R}^{m,1}$ is said to be *PH-preserving* or *MPH-preserving* respectively if, for every PH or MPH curve $\mathbf{r}(t)$ in $\mathbb{R}^n$ or $\mathbb{R}^{n,1}$, $\phi(\mathbf{r}(t))$ is also a PH or MPH curve in $\mathbb{R}^m$ or $\mathbb{R}^{m,1}$.

Example 2.1. Let $X = \mathbb{R}^3$ and let $\Psi \colon X \to X$ be the affine transformation given by

$$\Psi(\mathbf{p}) = \lambda \mathbf{R}\mathbf{p} + \mathbf{k} \quad \text{for } \forall \mathbf{p} \in X,$$

where $\mathbf{R}$ is an orthogonal matrix and $\mathbf{k}$ is a constant vector in X, and $\lambda \in \mathbb{R}\backslash\{0\}$ is a scaling factor. Then, for a PH curve $\mathbf{r}(t)$ in X, the mapping Ψ is PH-preserving, since

$$\begin{aligned} \langle \Psi(\mathbf{r}(t))', \Psi(\mathbf{r}(t))' \rangle &= \langle \lambda \mathbf{R}\mathbf{r}'(t), \lambda \mathbf{R}\mathbf{r}'(t) \rangle \\ &= \lambda^2 \langle \mathbf{r}'(t), \mathbf{r}'(t) \rangle \\ &= \lambda^2 \|\mathbf{r}'(t)\|_3^2, \end{aligned} \tag{1}$$

where $\langle \, , \rangle$ denotes the usual inner product in X. If $X = \mathbb{R}^{2,1}$, Eq. (1) shows that the affine transformation $\Psi \colon X \to X$ is MPH-preserving.

Let $\psi(u, v) = (x(u, v), y(u, v), z(u, v))$ be the polynomial mapping given by

$$x(u, v) = v - vu^2 - \frac{v^3}{3}, \;\; y(u, v) = -2uv, \;\; z(u, v) = -v - u^2 v - \frac{v^3}{3}.$$

Then, for any $\mathbf{r}(t) = (u(t), v(t))$ in $\mathbb{R}^{1,1}$, we obtain

$$\begin{aligned} \|\psi(\mathbf{r}(t))'\|_{2,1}^2 = \left(v' - 2uvu' - u^2 v' - v^2 v'\right)^2 + (2uu' + 2vv')^2 \\ - \left(v' + 2uvu' + u^2 v' + v^2 v'\right)^2 \end{aligned}$$

$$= 4v^2(u'^2 - v'^2) = 4v^2\|\mathbf{r}(t)'\|_{1,1}^2.$$

This shows that $\psi(u, v)$ is MPH-preserving.

Definition 2.3. A polynomial mapping $\phi\colon \mathbb{R}^n \to \mathbb{R}^{m,1}$ is said to be *PH-MPH transitive* if, for every PH curve $\mathbf{r}(t)$ in $\mathbb{R}^n$, $\phi(\mathbf{r}(t))$ is an MPH curve in $\mathbb{R}^{m,1}$.

Example 2.2. Let $\Phi\colon \mathbb{R}^2 \to \mathbb{R}^{2,1}$ be a polynomial mapping given by

$$\Phi(u, v) = (\sqrt{2}u - \frac{3}{\sqrt{2}}v, \sqrt{2}u + \frac{3}{\sqrt{2}}v, \sqrt{5}v).$$

Then the mapping Φ is PH-MPH transitive for any PH curve $\mathbf{r}(t) = (u(t), v(t))$ in $\mathbb{R}^2$, since

$$\begin{aligned}\langle \Phi(\mathbf{r}(t))', \Phi(\mathbf{r}(t))' \rangle &= \left(\sqrt{2}u' - \frac{3}{\sqrt{2}}v'\right)^2 + \left(\sqrt{2}u' + \frac{3}{\sqrt{2}}v'\right)^2 - (\sqrt{5}v')^2 \\ &= 4u'^2 + 9v'^2 - 5v'^2 \\ &= 4(u'^2 + v'^2),\end{aligned}$$

again $\langle\,,\rangle$ denotes the usual inner product in $\mathbb{R}^{2,1}$.

3. C^1 Hermite interpolation with MPH curves using PH-MPH transitive mappings

In 1983, Kobayashi [14] introduced the Weierstrass-Enneper representation of maximal surfaces, which are *space-like* surfaces with vanishing mean curvature in $\mathbb{R}^{2,1}$. He also introduced three interesting examples of maximal cubic surfaces: an Enneper surface of the 1st kind; an Enneper surface of the 2nd kind; and the conjugate of an Enneper surface of the 2nd kind. In this section, we will prove that the parameterizations of these surfaces are PH-MPH transitive, and show that we can solve C^1 Hermite interpolation problems with them.

3.1. Enneper surfaces in $\mathbb{R}^{2,1}$

Definition 3.1. Let $\Omega_k \in \mathbb{R}^{2,1}$ be an Enneper surface of the first kind with the parameterization $\Psi_k\colon \mathbb{R}^2 \to \mathbb{R}^{2,1}$ as follows:

$$\Psi_k(u, v) = k\left(\frac{u^3}{3} - uv^2 + u,\, -\frac{v^3}{3} + u^2v - v,\, v^2 - u^2\right), \tag{2}$$

where $k \in \mathbb{R}\setminus\{0\}$ is a constant. The Enneper surface of the 2nd kind $\Sigma_k \in \mathbb{R}^{2,1}$ has a parameterization $\Phi_k\colon \mathbb{R}^2 \to \mathbb{R}^{2,1}$, as follows:

$$\Phi_k(u, v) = k\left(\frac{u^3}{3} - uv^2 + u, -2uv, \frac{u^3}{3} - uv^2 - u\right), \text{ where } u \neq 0. \tag{3}$$

In addition, the conjugate of an Enneper surface of the 2nd kind, denoted by Σ_k^*, is parameterized by the mapping $\Phi_k^*\colon \mathbb{R}^2 \to \mathbb{R}^{2,1}$, as follows:

$$\Phi_k^*(u,v) = k\left(\frac{v^3}{3} - u^2 v - v, v^2 - u^2, \frac{v^3}{3} - u^2 v + v\right), \text{ where } u \neq 0. \tag{4}$$

The following theorem establishes that all the parameterizations of cubic Enneper surfaces commonly have the interesting property of converting PH curves in $\mathbb{R}^2$ to MPH curves in $\mathbb{R}^{2,1}$.

Theorem 3.1. *Ψ_k, Φ_k and Φ_k^* are PH-MPH transitive.*

Proof. If $\mathbf{r}(t) = (u(t), v(t))$ is a PH curve in $\mathbb{R}^2$, then, since

$$\begin{aligned}\|\Psi_k(\mathbf{r}(t))'\|_{2,1}^2 &= k^2\{(u^2u' - 2uvv' - v^2u' - u')^2 + (-v^2v' + 2uvu' + u^2v'v')^2 \\ &\qquad - (2vv' - 2uu')^2\} \\ &= k^2(u^2 + v^2 - 1)^2(u'^2 + v'^2),\end{aligned}$$

the curve $\Psi_k(\mathbf{r}(t))$ in $\mathbb{R}^{2,1}$ is an MPH curve. Furthers, since

$$\begin{aligned}\|\Phi_k(\mathbf{r}(t))'\|_{2,1}^2 &= k^2\{(u(t)^2u'(t) - u'(t)v(t)^2 - 2u(t)v(t)v'(t) + u'(t))^2 \\ &\qquad + (2u'(t)v(t) + 2u(t)v'(t))^2 \\ &\qquad - (u(t)^2u'(t) - u'(t)v(t)^2 - 2u(t)v(t)v'(t) - u'(t))^2\} \\ &= 4k^2u^2(u'^2 + v'^2),\end{aligned}$$

the curve $\Phi_k(\mathbf{r}(t))$ in $\mathbb{R}^{2,1}$ is also an MPH curve. In addition, since

$$\begin{aligned}\|\Phi_k^*(\mathbf{r}(t))'\|_{2,1}^2 &= k^2\{(v(t)^2v'(t) - v'(t)u(t)^2 - 2v(t)u(t)u'(t) - v'(t))^2 \\ &\qquad + (2v(t)v'(t) - 2u(t)u'(t))^2 \\ &\qquad - (v(t)^2v'(t) - v'(t)u(t)^2 - 2u(t)u'(t)v(t) + v'(t))^2\} \\ &= 4k^2u^2(u'^2 + v'^2),\end{aligned}$$

the curve $\Phi_k^*(\mathbf{r}(t))$ in $\mathbb{R}^{2,1}$ is yet another MPH curve. This completes the proof. □

Figure 1 shows the surfaces Ω_1, Σ_1 and Σ_1^* over the intervals $-1 \leq u \leq 1$ and $-1 \leq v \leq 1$. From this figure we can see that Ω_1 is very similar to a symmetrical Enneper surface in $\mathbb{R}^3$, but Σ_1 and Σ_1^* are severely twisted enough to be clearly distinguished from Ω_1. These observations suggest that Ω_1 might provide flexibility in a form more appropriate for solving C^1 Hermite interpolation problems than Σ_1 and Σ_1^*. These surfaces might reasonably be expected to be more restricted because of the singularity at $u = 0$, as well as their twisted shapes. Therefore, we will mainly experiment with Ω_k, and also Σ_k^*, equivalent to Ψ_k and Φ_k^*, in addressing C^1 Hermite interpolation problems in $\mathbb{R}^{2,1}$.

We now look more clearly at the applicability of Ω_k to interpolation problems. In the following theorem we will show that Ω_k contains certain straight

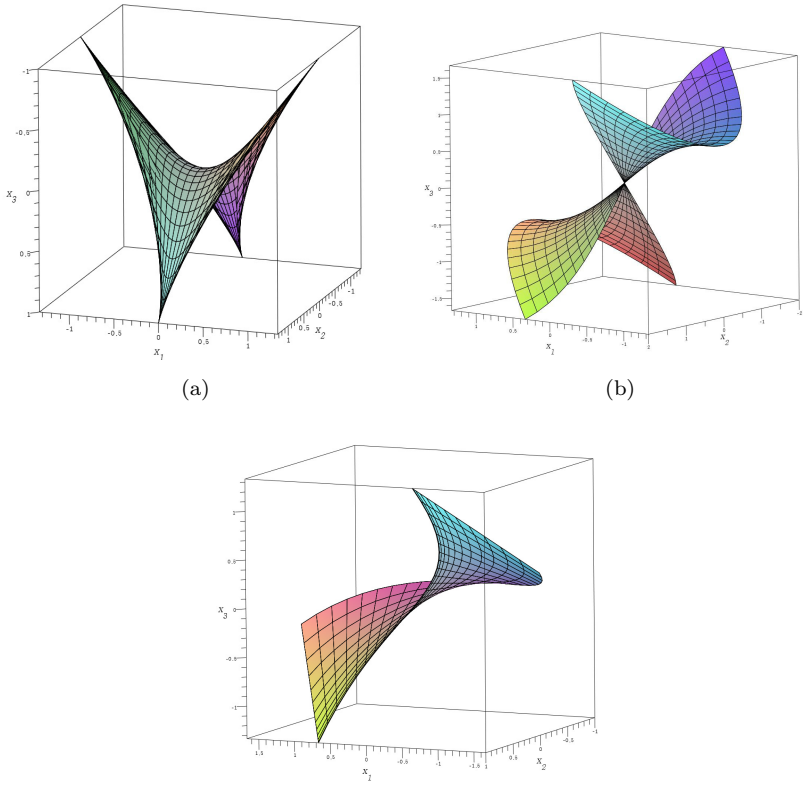

(a) (b)

(c)

FIGURE 1. Enneper surfaces over the intervals $-1 \leq u \leq 1$ and $-1 \leq v \leq 1$: (a) Ω_1; (b) Σ_1; (c) Σ_1^*. These surfaces are respectively parameterized by Ψ_k, Φ_k and Φ_k^*, when $k = 1$.

lines on the xy-plane in $\mathbb{R}^{2,1}$, which we can exploit in re-arranging data-sets to make them admissible for interpolation.

Theorem 3.2. *Ω_k contains the straight line $l_\omega^\pm = \{(x_1, x_2, x_3) \in \mathbb{R}^{2,1} \,|\, x_1 = \pm x_2,\ x_3 = 0\}$. At $\mathbf{p}_0 = (0,0,0) \in \Omega_k$, the xy-plane is tangent to Ω_k.*

Proof. Let $\mathbf{p}_0 = (x_1, x_2, x_3) \in \Omega_k$ and $x_3 = 0$. Then, from $x_3 = u^2 - v^2 = 0$, we obtain $u = \pm v$. Further, since

$$\Psi_k(u,v)|_{v=\pm u} = k\left(u - \frac{2u^3}{3}\right)(1, \mp 1, 0),$$

we can obtain $l_\omega^\pm = \{(x_1, x_2, x_3) \in \mathbb{R}^{2,1} \,|\, x_1 = \pm x_2, x_3 = 0\}$. Note that ${\Psi_k}^{-1}(0,0,0) = \left\{(0,0), (\frac{\sqrt{6}}{2}, \frac{\sqrt{6}}{2}), (-\frac{\sqrt{6}}{2}, -\frac{\sqrt{6}}{2}), (\frac{\sqrt{6}}{2}, -\frac{\sqrt{6}}{2}), (-\frac{\sqrt{6}}{2}, \frac{\sqrt{6}}{2})\right\} \subset \mathbb{R}^2$. Thus, when $u = v = 0$, since $\frac{\partial \Psi_k^*}{\partial u}(0,0,0) = (1,0,0)$ and $\frac{\partial \Psi_k^*}{\partial v}(0,0,0) = (0,-1,0)$, the xy-plane in $\mathbb{R}^{2,1}$ is tangent to Ω_k at $(0,0,0)$. This completes the proof. □

Example 3.1. Let $\mathbf{r}(t) = (t^2, \frac{t^3}{3} - t)$ and let $\mathbf{T}_\lambda(t)$ be the Tschirnhausen cubic $\big(3\lambda(t^2-3), at(t^3-3)\big)$. Then $\mathbf{r}(t) = \mathbf{T}_{\frac{1}{3}}(t) + (3,0)$ and $\|\mathbf{r}'(t)\|^2 = (2t)^2 + (t^2-1)^2 = (t^2+1)^2$. Hence $\mathbf{r}(t)$ is a PH curve in $\mathbb{R}^2$. Since Ψ_1, Φ_1 and Φ_1^* are all PH-MPH transitive, $\Psi_1(\mathbf{r}(t))$, $\Phi_1(\mathbf{r}(t))$ and ${\Phi_1}^*(\mathbf{r}(t))$, shown in Figure 2, are all MPH curves in $\mathbb{R}^{2,1}$. The figure suggests that, while $\Psi_1(\mathbf{r}(t))$ is good-shaped, $\Phi_1(\mathbf{r}(t))$ is likely to be the worst of these three interpolants because it has a singularity at $u = 0$. Φ_1^* has the same singularity, and the curve ${\Phi_1}^*(\mathbf{r}(t))$ passes through that singularity at $u = v = 0$ (i.e., when $t = 0$).

3.2. C^1 Hermite interpolation with MPH curves in $\mathbb{R}^{2,1}$ using Ψ_k

We now show how to solve C^1 Hermite interpolation problems in $\mathbb{R}^{2,1}$ using Ψ_k, which are MPH curves on the surfaces Ω_k, to reduce them to problems in $\mathbb{R}^2$.

Definition 3.2. A C^1 Hermite data-set $H_C^1 = \{\mathbf{p}_0, \mathbf{p}_1, \mathbf{v}_0, \mathbf{v}_1\}$ consists of two end-points $\mathbf{p}_0$ and $\mathbf{p}_1$, and two velocities $\mathbf{v}_0$ and $\mathbf{v}_1$ at those end-points, where $\mathbf{p}_1 - \mathbf{p}_0$, $\mathbf{v}_0$ and $\mathbf{v}_1 \in \mathbb{R}^{2,1}$ are all space-like, i.e., $\|\mathbf{p}_1 - \mathbf{p}_0\|_{2,1} > 0$, $\|\mathbf{v}_0\|_{2,1} > 0$ and $\|\mathbf{v}_1\|_{2,1} > 0$.

If $\mathbf{p}_0$ and $\mathbf{p}_1$ lie on a surface Σ, and $\mathbf{v}_0$ and $\mathbf{v}_1$ are tangents to that surface, then we can say that Σ satisfies H_C^1. If ϕ is a mapping which generates the surface Σ, then we can also say that ϕ satisfies H_C^1.

Definition 3.3. For a C^1 Hermite data-set $H_C^1 = \{\mathbf{p}_0, \mathbf{p}_1, \mathbf{v}_0, \mathbf{v}_1\}$, $H_{C^1}^s = \{\mathbf{p}_0^s, \mathbf{p}_1^s, \mathbf{v}_0^s, \mathbf{v}_1^s\}$ is called the *standard* data-set of H_C^1, when $\mathbf{p}_0$, $\mathbf{p}_1$, $\mathbf{v}_0$ and $\mathbf{v}_1$ can be respectively transformed to $\mathbf{p}_0^s = (0,0,0)$, $\mathbf{p}_1^s = (1,1,0)$ (or $(1,-1,0)$), $\mathbf{v}_0^s = (v_{01}, v_{02}, 0)$ and $\mathbf{v}_1^s = (v_{11}, v_{12}, v_{13})$, using a mapping composed of a translation, a rotation and a scaling.

Remark 3.1. We can find the standard data-set $H_{C^1}^s$ of any C^1 Hermite data-set $H_C^1 = \{\mathbf{p}_0, \mathbf{p}_1, \mathbf{v}_0, \mathbf{v}_1\}$, as follows: First, we translate $\mathbf{p}_0$ and $\mathbf{p}_1$ by $-\mathbf{p}_0$. Next we rotate the vectors $\mathbf{p}_1 - \mathbf{p}_0$, $\mathbf{v}_0$ and $\mathbf{v}_1$ together around the origin, until $\mathbf{p}_1 - \mathbf{p}_0$ is transformed to a vector on the straight line $x_1 = x_2$ or $x_1 = -x_2$. Then we rotate these transformed vectors around this line, until the transformed initial velocity vector becomes tangent to the xy-plane. Finally, we scale the transformed vectors together until the norm of the transformed vector which was on the straight line becomes $\sqrt{2}$. A C^1 Hermite data-set H_C^1 is *regular* if $\mathbf{p}_1^s = (1,1,0)$ (or $\mathbf{p}_1^s = (1,-1,0)$), $\mathbf{v}_0^s$ and $\mathbf{v}_1^s$ in $H_{C^1}^s$ are linearly independent; and then, obviously, $v_{13} \neq 0$. A data-set is *admissible* for interpolation when we can find interpolants that satisfy it.

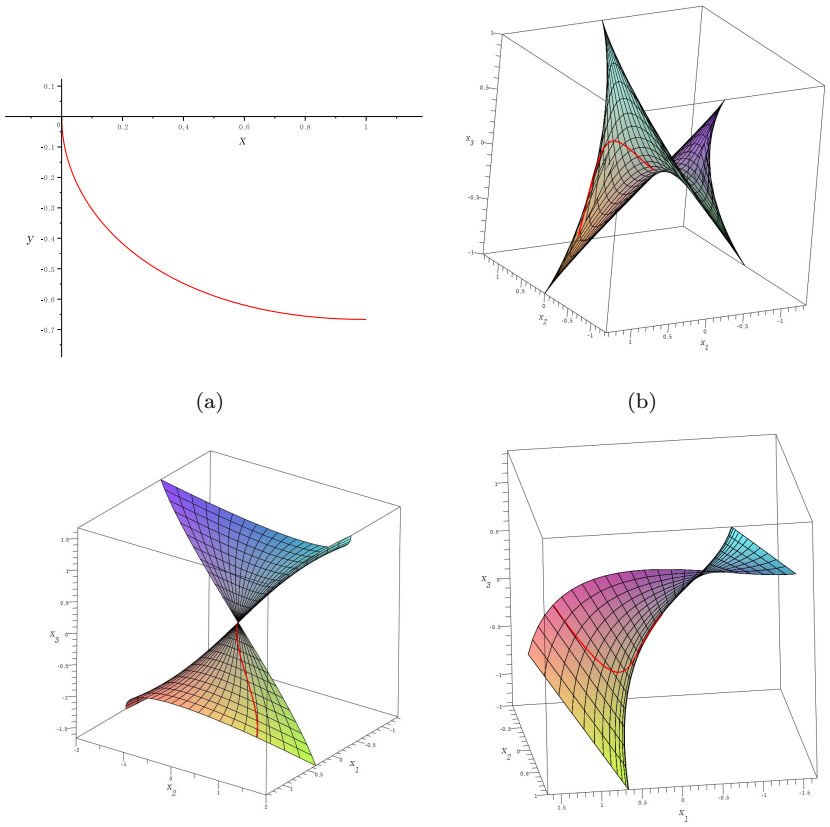

FIGURE 2. $\mathbf{r}(t)$ from Example 3.1, over the interval $0 \le t \le 1$, and images of the Enneper surfaces produced by the mappings Ψ_1, Φ_1 and Φ_1^* in $\mathbb{R}^{2,1}$: (a) $\mathbf{r}(t)$, (b) $\Psi_1(\mathbf{r}(t))$, (c) $\Phi_1(\mathbf{r}(t))$, and (d) $\Phi_1^*(\mathbf{r}(t))$.

The following two theorems give us the criteria necessary to determine whether a standardized regular C^1 Hermite data-set H_C^1 is admissible for our interpolation method.

Theorem 3.3. *For a regular C^1 Hermite data-set $H_{C^1}^s = \{(0,0,0),(1,1,0), \mathbf{v}_0^s = (v_{01}, v_{02}, 0), \mathbf{v}_1^s = (v_{11}, v_{12}, v_{13})\}$, if $|v_{11} - v_{12}| > \sqrt{2}|v_{13}|$, we can obtain eight generic MPH interpolants satisfying $H_{C^1}^s$, which lie on two Enneper surfaces of the 1st kind.*

Proof. Let Ω_k be an Enneper surface of the 1st kind, parameterized by Ψ_k, which is expressed by Eq. (2), and let $\alpha(t) = (u(t), v(t))$ $(0 \le t \le 1)$ be a PH

curve on $\mathbb{R}^2$ satisfying $\alpha(0) = (u(0), v(0)) = (0, 0)$ and $\alpha(t) = (u(1), v(1)) = (u_1, -u_1)$, with $u_1 \neq 0$. Then, since Ψ_k is PH-MPH transitive, $\Psi_k(\alpha(t))$ is an MPH curve on Ω_k. In order for this curve to satisfy the given data-set $H^s_{C^1}$, the following constraints must be satisfied:

$$\Psi_k(\alpha(0)) = (0, 0, 0), \quad \Psi_k(\alpha(1)) = (1, 1, 0), \tag{5}$$

$$\begin{aligned} \frac{d\Psi_k(\alpha(t))}{dt}|_{t=0} &= \frac{\partial \Psi_k}{\partial u}(\alpha(t))|_{t=0} u'(0) + \frac{\partial \Psi_k}{\partial v}(\alpha(t))|_{t=0} v'(0) \\ &= (v_{01}, v_{02}, 0), \end{aligned} \tag{6}$$

$$\begin{aligned} \frac{d\Psi_k(\alpha(t))}{dt}|_{t=1} &= \frac{\partial \Psi_k}{\partial u}(\alpha(t))|_{t=1} u'(1) + \frac{\partial \Psi_k}{\partial v}(\alpha(t))|_{t=1} v'(1) \\ &= (v_{11}, v_{12}, v_{13}). \end{aligned} \tag{7}$$

By, substituting $u(0) = 0, v(0) = 0$ and $u(1) = u_1, v(1) = -u_1$ into Eq. (2), we can readily show that Eq. (5) is satisfied when

$$k\left(u_1 - \frac{2u_1^3}{3}\right) = 1. \tag{8}$$

However, after this substitution, $\frac{\partial \Psi_k}{\partial u} = k(u^2 - v^2 + 1, 2uv, -2u)$ and $\frac{\partial \Psi_k}{\partial v} = k(-2uv, -v^2 + u^2 - 1, 2v)$, and thus the constraints of Eqs. (6) and (7) change to

$$\frac{d\Psi_k(\alpha(t))}{dt}|_{t=0} = k(1, 0, 0)u'(0) + k(0, -1, 0)v'(0) = (v_{01}, v_{02}, 0), \tag{9}$$

$$\begin{aligned} \frac{d\Psi_k(\alpha(t))}{dt}|_{t=1} &= k(1, -2u_1^2, -2u_1)u'(1) + k(2u_1^2, -1, -2u_1)v'(1) \\ &= (v_{11}, v_{12}, v_{13}). \end{aligned} \tag{10}$$

From Eq. (9) we obtain $u'(0) = \frac{v_{01}}{k}$ and $v'(0) = -\frac{v_{02}}{k}$, if $k \neq 0$.

To transform the original problem with the data-set $H^s_{C^1}$ in $\mathbb{R}^{2,1}$ to the problem searching for C^1 Hermite PH interpolants in $\mathbb{R}^2$, we have to find a value of u_1 that satisfies Eq. (10) for some $\mathbf{v}^s_1$ in $\mathbb{R}^{2,1}$. We start by obtaining the following equalities from Eq. (10):

$$ku'(1) + 2ku_1^2 v'(1) = v_{11}, \tag{11}$$

$$-2ku_1^2 u'(1) - kv'(1) = v_{12}, \tag{12}$$

$$-2ku_1 u'(1) - 2ku_1 v'(1) = v_{13}; \tag{13}$$

and from these we obtain $k(2u_1^2+1)(u'(1)+v'(1)) = v_{11} - v_{12}$ and $-2k(u'(1)+v'(1))u_1 = v_{13}$. If we recall that $v_{13} \neq 0$, since $H^s_{C^1}$ is regular, we see that eliminating the term $(u'(1) + v'(1))$ from Eqs. (11)-(13) yields a quadratic equation for u_1:

$$2v_{13}u_1^2 + 2(v_{11} - v_{12})u_1 + v_{13} = 0. \tag{14}$$

If $|v_{11} - v_{12}| > \sqrt{2}|v_{13}|$, we can obtain two distinct real roots which satisfy this equation. Substituting one of these values for u_1 into Eq. (8), we can

obtain a generic value of k which satisfies it, except in the singular case where $u_1 = \pm\sqrt{\frac{3}{2}}$. Finally, substituting these values for u_1 and k, we can solve Eqs. (12) and (13) simultaneously, and hence obtain $u'(1)$ and $v'(1)$.

We have now achieved our aim of reducing the original interpolation problem to a C^1 Hermite interpolation problem in $\mathbb{R}^2$, with the data-set $H^p_{C^1} = \{(0,0),(u_1,-u_1),(u'(0),v'(0)),(u'(1),v'(1))\}$. Since we can always [7] find four PH quintic interpolants in $\mathbb{R}^2$ for a regular C^1 Hermite data-set $H^p_{C^1}$, we can obtain four MPH interpolants on the Enneper surface Ω_k given by $\Psi_k(\alpha(t))$, where $\alpha(t)$ is the PH quintic that satisfies $H^p_{C^1}$ in $\mathbb{R}^2$. Since Eq. (14) has two distinct real roots, we can obtain eight MPH interpolants satisfying $H^s_{C^1}$ on two Enneper surfaces of the 1st kind, provided only that $|v_{11} - v_{12}| > \sqrt{2}|v_{13}|$. □

Theorem 3.4. *For a regular C^1 Hermite data-set $H^s_{C^1} = \{(0,0,0),(1,-1,0), \mathbf{v}^s_0 = (v_{01},v_{02},0),\ \mathbf{v}^s_1 = (v_{11},v_{12},v_{13})\}$, if $|v_{11}+v_{12}| > \sqrt{2}|v_{13}|$, we can obtain eight generic MPH interpolants satisfying $H^s_{C^1}$, which lie on two Enneper surfaces of the 1st kind.*

Proof. This is similar to the proof of the previous theorem. Let Ω_k be an Enneper surface of the 1st kind, parameterized by Ψ_k, formulated in Eq. (2), and let $\beta(t) = (u(t),v(t))$ $(0 \le t \le 1)$ be a PH curve on $\mathbb{R}^2$ which satisfies $\beta(0) = (u(0),v(0)) = (0,0)$ and $\beta(t) = (u(1),v(1)) = (u_1,u_1)$ when $u_1 \neq 0$. Then, since Ψ_k is PH-MPH transitive, $\Psi_k(\beta(t))$ is also an MPH curve on Ω_k. If we assume that the curve $\Psi_k(\beta(t))$ satisfies $H^s_{C^1}$, then we obtain the following:

$$\Psi_k(\beta(0)) = (0,0,0), \qquad \Psi_k(\beta(1)) = (1,-1,0), \tag{15}$$

$$\begin{aligned}\frac{d\Psi_k(\beta(t))}{dt}|_{t=0} &= \frac{\partial\Psi_k}{\partial u}(\beta(t))|_{t=0}u'(0) + \frac{\partial\Psi_k}{\partial v}(\beta(t))|_{t=0}v'(0)\\ &= (v_{01},v_{02},0),\end{aligned} \tag{16}$$

$$\begin{aligned}\frac{d\Psi_k(\beta(t))}{dt}|_{t=1} &= \frac{\partial\Psi_k}{\partial u}(\beta(t))|_{t=1}u'(1) + \frac{\partial\Psi_k}{\partial v}(\beta(t))|_{t=1}v'(1)\\ &= (v_{11},v_{12},v_{13}).\end{aligned} \tag{17}$$

By substituting $u(0) = 0, v(0) = 0$ and $u(1) = u_1, v(1) = u_1$ into Eq. (2), we can confirm that Eq. (15) is satisfied if Eq. (8) holds. Making the same substitution in Eqs. (16) and (17) yields

$$\frac{d\Psi_k(\beta(t))}{dt}|_{t=0} = k(1,0,0)u'(0) + k(0,-1,0)v'(0) = (v_{01},v_{02},0), \tag{18}$$

$$\begin{aligned}\frac{d\Psi_k(\beta(t))}{dt}|_{t=1} &= k(1,2u_1^2,-2u_1)u'(1) + k(-2u_1^2,-1,2u_1)v'(1)\\ &= (v_{11},v_{12},v_{13}).\end{aligned} \tag{19}$$

From Eq. (18) we obtain $u'(0) = \frac{v_{01}}{k}$ and $v'(0) = -\frac{v_{02}}{k}$ if $k \neq 0$, as in the previous proof. We can also obtain a value of u_1 which satisfies Eq. (19) for

some $\mathbf{v}_1^s$ in $\mathbb{R}^{2,1}$, again following the previous proof. From Eq. (10) we obtain the following:

$$ku'(1) - 2ku_1^2 v'(1) = v_{11}, \tag{20}$$

$$2ku_1^2 u'(1) - kv'(1) = v_{12}, \tag{21}$$

$$-2ku_1 u'(1) + 2ku_1 v'(1) = v_{13}. \tag{22}$$

From these equations we obtain $k(2u_1^2 + 1)(u'(1) - v'(1)) = v_{11} + v_{12}$ and $-2k(u'(1) - v'(1))u_1 = v_{13}$. Also, since $v_{13} \neq 0$, we can eliminate the term $(u'(1) - v'(1))$ from Eqs. (20)-(22), we finally obtain

$$2v_{13}u_1^2 + 2(v_{11} + v_{12})u_1 + v_{13} = 0. \tag{23}$$

Thus, if $|v_{11} + v_{12}| > \sqrt{2}|v_{13}|$, except in the singular case where $u_1 = \pm\sqrt{\frac{3}{2}}$, we can obtain two distinct real roots which satisfy this equation. Thus we have again reduced the original interpolation problem to a C^1 Hermite interpolation problem in $\mathbb{R}^2$, with the data-set $H_{C^1}^p = \{(0,0), (u_1, u_1), (u'(0), v'(0)), (u'(1), v'(1))\}$. And again this means that, if $|v_{11}+v_{12}| > \sqrt{2}|v_{13}|$, we can obtain eight MPH interpolants satisfying $H_{C^1}^s$ on two Enneper surfaces of the 1st kind. □

Remark 3.2. We should consider what happens when $|v_{11} - v_{12}| = \sqrt{2}|v_{13}|$ or $|v_{11} + v_{12}| = \sqrt{2}|v_{13}|$. In these cases, Eqs. (14) and (23) usually have one real root, which is $\frac{1}{\sqrt{2}}$ or $-\frac{1}{\sqrt{2}}$. However, if $v_{11} = -v_{12} = \pm\frac{v_{13}}{\sqrt{2}}$ in the first case, and if $v_{11} = v_{12} = \pm\frac{v_{13}}{\sqrt{2}}$ in the second, we cannot find suitable values of $u'(1)$ and $v'(1)$ to satisfy Eqs. (7) and (19) respectively. And thus, we cannot reduce an interpolation problem with MPH curves in $\mathbb{R}^{2,1}$ to a problem in $\mathbb{R}^2$. However, even though Eq. (7) or Eq. (19) has real solutions, these cases are singularities which only occur when $\mathbf{v}_1^s = (\pm\frac{v_{13}}{\sqrt{2}}, \mp\frac{v_{13}}{\sqrt{2}}, v_{13})$ and $\mathbf{v}_1^s = (\pm\frac{v_{13}}{\sqrt{2}}, \pm\frac{v_{13}}{\sqrt{2}}, v_{13})$ respectively, for any given v_{13}.

Remark 3.3. Let $D_1 = \{(x_1, x_2, x_3) \in \mathbb{R}^{2,1} \mid |x_1 - x_2| > \sqrt{2}|x_3|\}$, $D_2 = \{(x_1, x_2, x_3) \in \mathbb{R}^{2,1} \mid |x_1 + x_2| > \sqrt{2}|x_3|\}$. Then, from the previous two theorems, we see that the standardized data-set of a regular C^1 Hermite data-set, $H_{C^1}^s = \{\mathbf{p}_0^s, \mathbf{p}_1^s, \mathbf{v}_0^s, \mathbf{v}_1^s\}$, is admissible if and only if $\mathbf{v}_1^s \in D_1$ when $\mathbf{p}_1^s = (1, 1, 0)$, or $\mathbf{v}_1^s \in D_2$ when $\mathbf{p}_1^s = (1, -1, 0)$. The regions of admissible values of the end velocity vectors can be indirectly visualized represented by using the projection $\pi : (x_1, x_2, x_3) \mapsto (x_1, x_2)$, with the results shown in Figure 3. According to this figure, for a point in the x_1x_2-plane, it seems that there can be two possibilities for admissibility. Here note that they are not freely optional but alternative for a regular C^1 Hermite data-set, depending on whether we choose $\mathbf{p}_1^s = (1, 1, 0)$ or $(1, -1, 0)$. However, when solving the interpolation problems with MPH biarcs for two admissible data-sets with an appropriate junction-point and its velocity vector as in Example 3.3, they can be freely optional.

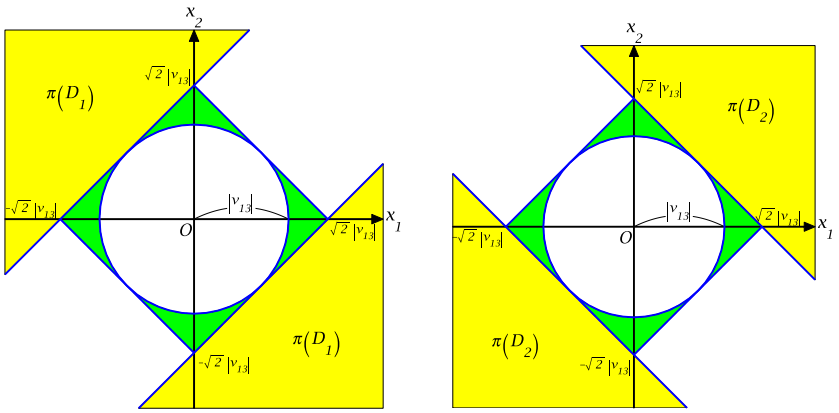

(a) (b)

FIGURE 3. Projection of the region of $\mathbf{v}_1^s$ into the x_1x_2-plane, for a fixed value of v_{13}, when $H_{C^1}^s$ is regular: (a) $\pi(D_1)$; (b) $\pi(D_2)$. The green region represents $\pi(D_1^c \cap D_2^c)$.

Example 3.2. Let $H_{C^1}^s = \{(0,0,0),(1,1,0),\mathbf{v}_0^s = (1,2,0),\mathbf{v}_1^s = (1,5,-2)\}$. Then, since $|v_{11} - v_{12}| > \sqrt{2}|v_{13}|$, Eq. (14) has two distinct solutions $u_1 = -0.2761423750, -1.707106781$. Using Theorem 3.3, we can obtain eight interpolants on two Enneper surfaces of the 1st kind, shown in Fig. 4(a) and (b): Each of them is obtained by means of a parametrization $\Psi_k(\alpha(t))$, where each $\alpha(t)$ is a PH quintic interpolant, shown in Fig. 5(a) and (b), satisfying the data-set $H_{C^1}^{p_1} = \Psi^{-1}(H_{C^1}^s)$ in $\mathbb{R}^2$. Next, since $|v_{11}+v_{12}| > \sqrt{2}|v_{13}|$, Eq. (23) has two distinct solutions $u_1 = 0.177124344$, 2.822875656. Thus, using Theorem 3.4, we can obtain eight interpolants on two Enneper surfaces of the 1st kind, satisfying $H_{C^1}^{\tilde{s}} = \{(0,0,0),\ (1,-1,0),\ \mathbf{v}_0^s = (1,2,0),\ \mathbf{v}_1^s = (1,5,-2)\}$, as shown in Fig. 4(c) and (d): Each of them is obtained using parametrization $\Psi_k(\beta(t))$, where each $\beta(t)$ is a PH quintic interpolant, shown in Fig. 5(c) and (d), satisfying the data-set $H_{C^1}^{p_2} = \Psi_k^{-1}(H_{C^1}^{\tilde{s}})$ in $\mathbb{R}^2$.

Comparing Figures 4 and 5, we find that the interpolants with good shape in $\mathbb{R}^{2,1}$ are mainly obtained from the C-shaped PH quintic interpolants with the lowest bending energy in $\mathbb{R}^2$. However, when the velocity vectors of $H_{C^1}^{p_i}$ are nearly parallel, the interpolant with the best shape is obtained by the S-shaped simple PH quintic interpolant in $\mathbb{R}^2$. We also observe that the interpolants satisfying $H_{C^1}^s$ ($H_{C^1}^{\tilde{s}}$) on Ω_k, corresponding one-to-one with these obtained using Ψ_k, have the same topologies shapes as the PH quintic interpolants satisfying $H_{C^1}^{p_1}$ ($H_{C^1}^{p_2}$) in $\mathbb{R}^2$, respectively.

To assess the fairness of interpolants more objectively, we introduce a measure of bending energy $\varepsilon = \int_\gamma \kappa^2 ds$, where $\gamma(s)$ is a planar curve parameterized

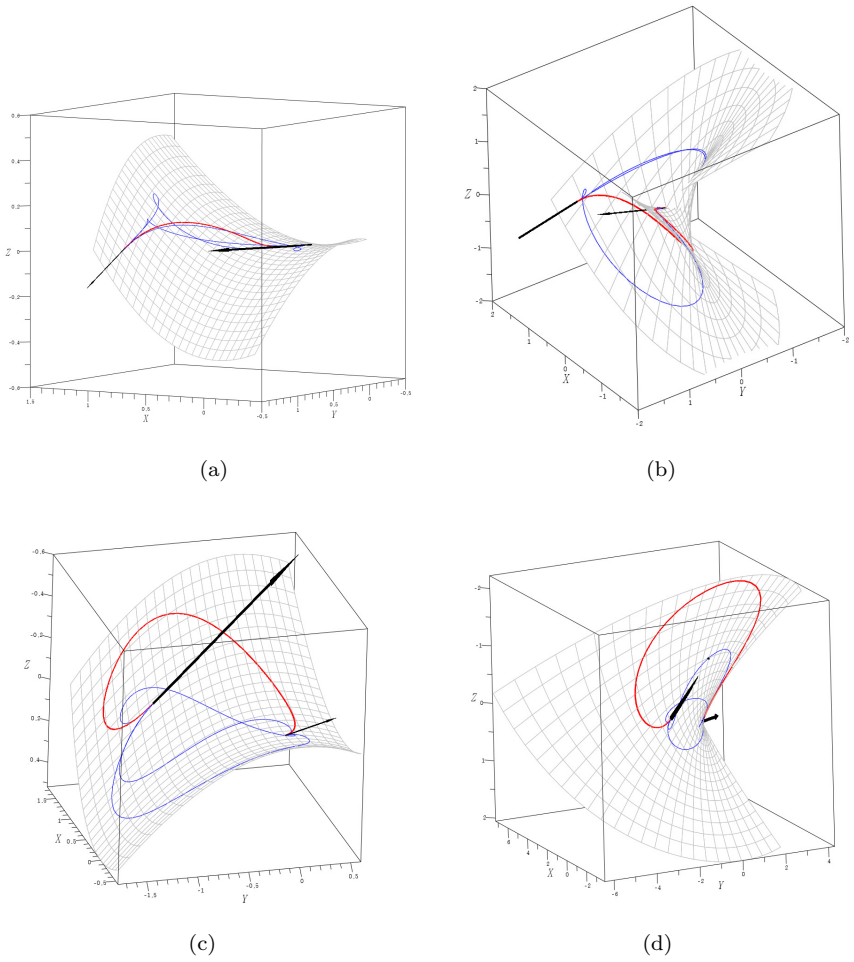

(a) (b)

(c) (d)

FIGURE 4. MPH interpolants satisfying $H^{s}_{C^1}$ and $H^{\tilde{s}}_{C^1}$ in Example 3.2: (a) four MPH interpolants satisfying $H^{s}_{C^1}$ on Ω_k, obtained using Ψ_k when $u_1 = -0.2761423750$; (b) four MPH interpolants satisfying $H^{s}_{C^1}$ on Ω_k, obtained using Ψ_k when $u_1 = -1.707106781$; (c) four MPH interpolants satisfying $H^{\tilde{s}}_{C^1}$ on Ω_k, obtained using Ψ_k when $u_1 = 0.177124344$; and (d) four MPH interpolants satisfying $H^{\tilde{s}}_{C^1}$ on Ω_k, obtained using Ψ_k when $u_1 = 2.822875656$. The interpolants drawn in red are obtained by applying the mapping Ψ_k to the corresponding red interpolants in Figure 5, which are those with the lowest bending energy.

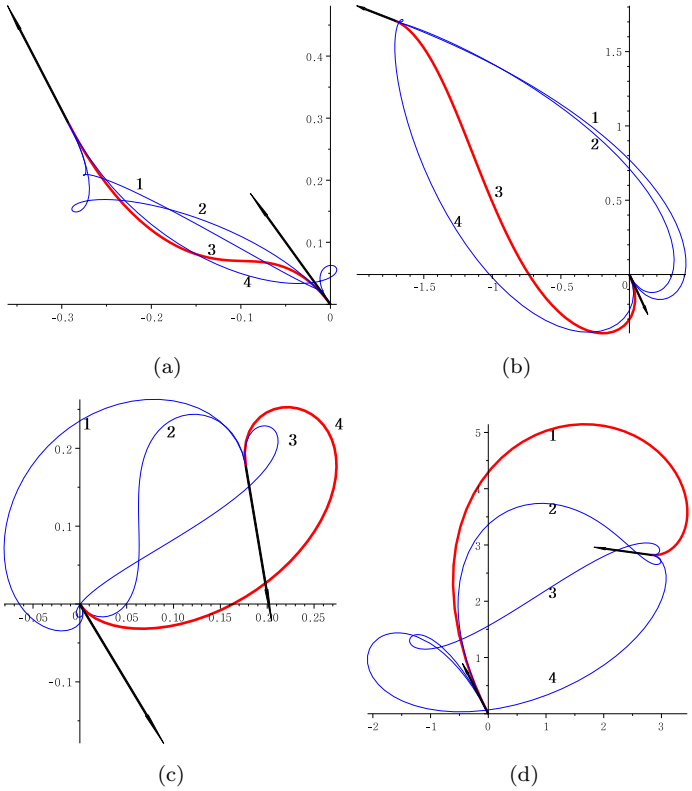

FIGURE 5. PH quintic interpolants in $\mathbb{R}^2$ satisfying $H^{p_1}_{C^1}$ and $H^{p_2}_{C^1}$ in Example 3.2: (a) four PH quintic interpolants satisfying $H^{p_1}_{C^1}$ in $\mathbb{R}^2$ when $u_1 = -0.2761423750$; (b) four PH quintic interpolants satisfying $H^{p_1}_{C^1}$ in $\mathbb{R}^2$ when $u_1 = -1.707106781$; (c) four PH quintic interpolants satisfying $H^{p_2}_{C^1}$ in $\mathbb{R}^2$ when $u_1 = 0.177124344$; and (d) four PH quintic interpolants satisfying $H^{p_2}_{C^1}$ in $\mathbb{R}^2$ when $u_1 = 2.822875656$. The interpolants drawn in red are those with the lowest bending energy for that value of u_1.

by arc length s, and $\kappa(s)$ is the curvature of $\gamma(s)$. In general, low bending energy and short arc length are both desirable properties of interpolants. Either of the interpolants shown in red in Figure 5(a)-(d) has the lowest bending energy. Then, in this case, as shown in Table 1, since the lowest values of arc-length is achieved at a high cost in terms of bending energy in most cases, we select the interpolant shown in red in Figure 5(a) as the best: it has not only fairly lower bending energy but also the shortest arc-length among all the

interpolants (see Table 1). Finally, according to this suggested perspective,

TABLE 1. Comparison of the bending energies and arc-lengths of the interpolants shown in Fig. 5.

Curves in (a)	Energy	Arc-length	Curves in (b)	Energy	Arc-length
(1)	51264.476	**0.443**	(1)	13.327	3.428
(2)	584.398	0.518	(2)	837637.659	**3.224**
(3)	**17.183**	**0.443**	(3)	**11.488**	**3.224**
(4)	441.210	0.518	(4)	460.304	3.428
Curves in (c)	Energy	Arc-length	Curves in (d)	Energy	Arc-length
(1)	25.356	3.605	(1)	**47.534**	15.474
(2)	34.284	2.594	(2)	276.633	6.473
(3)	197.006	**2.483**	(3)	387.380	**3.351**
(4)	**18.042**	3.573	(4)	259.682	4.085

it seems to be reasonable to consider each of the interpolants shown in red in Figure 4(a) and (c) to be the best MPH interpolant, respectively satisfying the original data-set $H^{s}_{C^1}$ and $H^{\tilde{s}}_{C^1}$.

This example also shows that, for a single admissible terminal velocity vector in the regular standard data-set of a C^1 Hermite data-set, either Theorem 3.3 or 3.4 alone can produce interpolants. But this does not mean that we can use the PH-MPH transitive mapping Ψ_k to obtain a possible total of 16 interpolnats lying on Enneper surfaces of the 1st kind from a single regular Hermite data-set. When the terminal velocity vector $\mathbf{v}_1^s$ is such that Theorems 3.3 and 3.4 are both applicable, each theorem works on a different C^1 Hermite data-set in $\mathbb{R}^{2,1}$, corresponding respectively to the standard data-set $H^{s}_{C^1} = \{(0,0,0),(1,1,0),\mathbf{v}_0^s,\mathbf{v}_1^s\}$ and $H^{s\star}_{C^1} = \{(0,0,0),(1,-1,0),\mathbf{v}_0^{s\star},\mathbf{v}_1^s\}$.

So why is it not possible to obtain 16 MPH interpolants satisfying a single data-set in this situation? Of course, reducing the original data-set to one of the standard data-sets $H^{s}_{C^1}$ or $H^{s\star}_{C^1}$ does not prevent us from obtaining another data-set by rotating the velocity vectors of the reduced data-set through $\frac{\pi}{2}$ or $-\frac{\pi}{2}$. If the velocity vectors of the reduced data-set are (v_{01},v_{02},v_{03}) and (v_{11},v_{12},v_{13}), then we can construct a new data-set with velocity vectors $(v_{02},-v_{01},v_{03})$ and $(v_{12},-v_{11},v_{13})$. However, an Enneper surface of the 1st kind Ω_k parameterized by Ψ_k is symmetrical under a rotation through $\frac{\pi}{2}$ or $-\frac{\pi}{2}$ around the x_3-axis. So the new set of eight interpolants will coincide with the original set, and we have created no extra interpolants.

Remark 3.4. Recall that $\mathbf{v}_1^s$ should be space-like, i.e., $\mathbf{v}_1^s \in \Delta = \{(x_1,x_2,x_3) \in \mathbb{R}^{2,1} \mid x_1^2 + x_2^2 > x_3^2\}$. Figure 3 suggests that, for any particular value of v_{13}, $\pi(D_1)\bigcup\pi(D_2)$ covers most of $\pi(\Delta)$, except in the case when $\mathbf{v}_1^s \in \mathcal{S} = \Delta \setminus D_1 \bigcup D_2$ (the green region in Figure 3). But, what if $\mathbf{v}_1^s \in \mathcal{S}$? In this case, our method does not work since $\mathbf{v}_1^s$ is not admissible. Does that mean that $\mathbf{v}_1^s$

is not admissible only when $\mathbf{v}_1^s \in \mathcal{S}$ throughout $\mathbb{R}^{2,1}$? Then, other singularities are possible: $\mathbf{v}_1^s \in \Delta \bigcap D_1^c$ when $\mathbf{p}_1 = (1,1,0)$, and $\mathbf{v}_1^s \in \Delta \bigcap D_2^c$ when $\mathbf{p}_1 = (1,-1,0)$. For these situations, we propose constructing a piecewise interpolant with two segments [15]. First, we assume that the regular standardized data-set $H_{C^1}^s$ of a C^1 Hermite data-set H_C^1 has a singular space-like terminal velocity vector $\mathbf{v}_1^s = (v_{11}, v_{12}, v_{13})$: for example, any $\mathbf{v}_1^s \in \mathcal{S}$. Next, assuming $\mathbf{p}_1 = (1,1,0)$, we introduce a suitable junction-point $\mathbf{p}_*$ near the line-segment between $\mathbf{p}_0 = (0,0,0)$ and $\mathbf{p}_1 = (1,1,0)$, and also a space-like velocity vector $\mathbf{v}_*$ which is admissible for our method, for example $\mathbf{v}_* \in \mathcal{D}$. Then we can obtain two new C^1 Hermite data-sets $H_{C^1}^1 = \{\mathbf{p}_0 = (0,0,0), \mathbf{p}_*, \mathbf{v}_0, \mathbf{v}_*\}$ and $H_{C^1}^2 = \{\mathbf{p}_*, \mathbf{p}_1, \mathbf{v}_*, \mathbf{v}_1\}$. We can easily transform $H_{C^1}^1$ to the standardized data-set $H_{C^1}^{1s}$ by rotating it around the z-axis in $\mathbb{R}^{2,1}$ and scaling. Then we can readily obtain MPH interpolants satisfying $H_{C^1}^{1s}$ using Theorem 3.3 and 3.4. If we can also standardize $H_{C^1}^2$ so that it can undergo simple transformations such as rotation, translation and scaling, which preserve the MPH property, then we can obtain MPH interpolants satisfying $H_{C^1}^{2s}$, again using Theorems 3.3 and 3.4. Then, by joining two interpolants which respectively satisfy $H_{C^1}^1$ and $H_{C^1}^2$, we can obtain MPH interpolants which satisfy the original C^1 Hermite data-set $H_{C^1}^s$. The following example illustrates this approach.

Example 3.3. Consider a inadmissible standard C^1 Hermite data-set $H_{C^1}^s = \{(0,0,0), (1,1,0), \mathbf{v}_0^s = (1,0,0), \mathbf{v}_1^s = (1,0.5,0.5)\}$. Note that $\mathbf{v}_1^s \in \Delta \bigcap D_1^c$ and $\mathbf{p}_1^s = (1,1,0)$. Now we introduce a junction-point $\mathbf{p}_* = (\frac{\sqrt{3}}{\sqrt{3}+1}, \frac{1}{\sqrt{3}+1}, 0)$ and a velocity vector $\mathbf{v}_* = (1, \frac{1}{2}, \frac{1}{8})$ at $\mathbf{p}_*$. Then, as discussed above, we can obtain two regular C^1 Hermite data-sets $H_{C^1}^1 = \{(0,0,0), \mathbf{p}_*, \mathbf{v}_0^s = (1,0,0), \mathbf{v}_*\}$ and $H_{C^1}^2 = \{\mathbf{p}_*, (1,1,0), \mathbf{v}_*, \mathbf{v}_1^s = (1,0.5,0.5)\}$. Since $\mathbf{v}_*$ is admissible, the former is easily transformed to an admissible standard data-set $H_{C^1}^{1s}$ by suitable rotation and scaling. It is more complicated to standardize the data-set $H_{C^1}^2$; but it can be achieved by a Euclidean rotation which makes the vector $\mathbf{p}_1^s - \mathbf{p}_*$ parallel to $(1,1,0)$, and followed by a hyperbolic rotation which makes the initial velocity vector tangent to the xy-plane. There are followed by a translation such that $\mathbf{p}_* \mapsto (0,0,0)$ and a scaling such that $\|\mathbf{p}_1^s - \mathbf{p}_*\| \mapsto \sqrt{2}$. These produce a standard data-set $H_{C^1}^{2s} = \{\mathbf{p}_*^s = (0,0,0), \mathbf{p}_1^s = (1,1,0), \mathbf{v}_*^s = (0.933, 0.250, 0), \mathbf{v}_1^{\tilde{s}} = (0.8080, 0.7165, 0.0604)\}$. Note that $\mathbf{v}_1^{\tilde{s}} = (0.8080, 0.7165, 0.0604)$ is admissible. Thus we can use Theorem 3.3 to obtain eight interpolants satisfying $H_{C^1}^{1s}$ and eight more that satisfy $H_{C^1}^{2s}$. Applying the inverse of the transformation used to standardize the data-sets, we can finally obtain 64 interpolants, in pairs, each of which meet with C^1 continuity at the junction-point $\mathbf{p}_*$, and satisfy the original data-set $H_{C^1}^s$, as shown in Figure 6(a).

We can now try to select the interpolant with the best-shape. The eight interpolants on each Ω_k have three types of shape: a C-shape an S-shape or a loop. We discard the loops at once, and compare the bending energies ε of the planar PH interpolants corresponding to the remaining MPH interpolants, as

we did in Example 3.2. The interpolant with best shape can be considered to be that formed from the two simple PH quintic segments with the lowest total bending energy from each of the sets of quintics which respectively satisfy the data-sets $H^{p_1}_{C^1} = \Psi_k^{-1}(H^{1s}_{C^1})$ and $H^{p_2}_{C^1} = \Psi_k^{-1}(H^{2s}_{C^1})$ in $\mathbb{R}^2$. There are shown in Figure 6 (b).

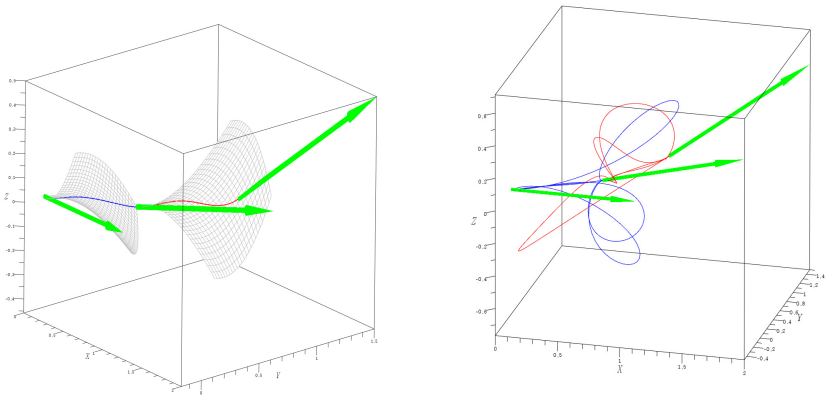

(a) (b)

FIGURE 6. MPH interpolants which pass through the junction-point $\mathbf{p}_* = (\frac{\sqrt{3}}{\sqrt{3}+1}, \frac{1}{\sqrt{3}+1}, 0)$ with C^1 continuity, and satisfy $H^s_{C^1}$ in Example 3.3: (a) the best-shaped MPH interpolant satisfying $H^s_{C^1}$; (b) 16 MPH interpolants on two Enneper surfaces of the 1st kind satisfying $H^s_{C^1}$ containing the best-shaped MPH interpolant. The interpolants satisfying $H^1_{C^1}$ are drown in blue, and these satisfying $H^2_{C^1}$ in red.

Remark 3.5. Note that, even though we can obtain some interpolants with good shape as shown in Figure 6, the process of standardizing the given data-set seems fairly complicated, as stated in Remark 3.4. Hence, it seems interesting to compare these interpolants with the ones obtained by existing methods for the same data-set, including the processes of dealing with data-sets, which seems to be a good theme in future work for utilization.

4. Conclusions and suggestions for further study

We have introduced PH-MPH transitive mappings which transform planar PH curves to MPH curves in $\mathbb{R}^{2,1}$, and proved the parameterizations of Enneper surfaces of the 1st and the 2nd kind and conjugates of Enneper surfaces of the 2nd kind are PH-MPH transitive. We showed how to solve C^1 Hermite interpolation problems in $\mathbb{R}^{2,1}$, for admissible C^1 Hermite data-sets, using a parametrization of Enneper surface of the 1st kind, and proved that we can

generically obtain eight interpolants which satisfy the data-set on two such surfaces. We also showed, by means of an example, that piecewise interpolants can satisfy some inadmissible data-sets.

The results obtained in this paper and some topics related to them raise further questions, in particular regarding inadmissible data-sets. Does the method using MPH biarcs always work and, if so, can we prove it? Or can we find other PH-MPH transitive mappings to replace Ψ_k, including Φ_k and Φ_k^*, for which all terminal velocity vectors are admissible? It seems that it might be possible to make better use of the mapping Φ_k^*, since the surface Σ_k^* parameterized by Φ_k^* is also a ruled surface [14], as Ω_k does.

The answers to more general questions require a thorough understanding of PH-MPH transitive mappings, which also merit further study. What makes a polynomial mapping PH-MPH transitive? And can we characterize all the possible polynomial PH-MPH transitive mappings of a given degree in terms of geometric properties such as their relationship to parameterizations of Enneper surfaces? Answering these questions for quadratic and cubic mappings, except parameterizations of Enneper surfaces, could be a feasible goal for a research project. Finally, from the viewpoint of practical utility in application, it is also important to focus intensively on the mappings which directly map spatial PH curves into spatial MPH curves and their use in interpolation problems.

References

[1] G. Albrecht and R. T. Farouki, *Construction of C^2 Pythagorean-hodograph interpolating splines by the homotopy method*, Adv. Comput. Math. **5** (1996), no. 4, 417–442.

[2] H. I. Choi, S. W. Choi, and H. P. Moon, *Mathematical theory of medial axis transform*, Pacific J. Math. **181** (1997), no. 1, 57–88.

[3] H. I. Choi, D. S. Lee, and H. P. Moon, *Clifford algebra, spin representation, and rational parameterization of curves and surfaces*, Adv. Comput. Math. **17** (2002), no. 1-2, 5–48.

[4] R. T. Farouki, *Pythagorean-hodograph curves*: *algebra and geometry inseparable*, Geometry and Computing, **1**, Springer, Berlin, 2008.

[5] R. T. Farouki, C. Manni, M. L. Sampoli, and A. Sestini, *Shape-preserving interpolation of spatial data by Pythagorean-hodograph quintic spline curves*, IMA J. Numer. Anal. **35** (2015), no. 1, 478–498.

[6] R. T. Farouki, C. Manni, and A. Sestini, *Shape-preserving interpolation by G^1 and G^2 PH quintic splines*, IMA J. Numer. Anal. **23** (2003), no. 2, 175–195.

[7] R. T. Farouki and C. A. Neff, *Hermite interpolation by Pythagorean hodograph quintics*, Math. Comp. **64** (1995), no. 212, 1589–1609.

[8] R. T. Farouki, F. Pelosi, M. L. Sampoli, and A. Sestini, *Tensor-product surface patches with Pythagorean-hodograph isoparametric curves*, IMA J. Numer. Anal. **36** (2016), no. 3, 1389–1409.

[9] R. T. Farouki and T. Sakkalis, *Pythagorean hodographs*, IBM J. Res. Develop. **34** (1990), no. 5, 736–752.

[10] R. T. Farouki and Z. Šìr, *Rational Pythagorean-hodograph space curves*, Comput. Aided Geom. Design **28** (2011), no. 2, 75–88.

[11] Z. Habib and M. Sakai, *G^2 Pythagorean hodograph quintic transition between two circles with shape control*, Comput. Aided Geom. Design **24** (2007), no. 5, 252–266.

[12] G. Jaklič, J. Kozak, M. Krajnc, V. Vitrih, and E. Žagar, *On interpolation by planar cubic G^2 Pythagorean-hodograph spline curves*, Math. Comp. **79** (2010), no. 269, 305–326.
[13] G.-I. Kim and S. Lee, *Pythagorean-hodograph preserving mappings*, J. Comput. Appl. Math. **216** (2008), no. 1, 217–226.
[14] O. Kobayashi, *Maximal surfaces in the 3-dimensional Minkowski space L^3*, Tokyo J. Math. **6** (1983), no. 2, 297–309.
[15] J. H. Kong, S. P. Jeong, S. Lee, and G. Kim, *C^1 Hermite interpolation with simple planar PH curves by speed reparametrization*, Comput. Aided Geom. Design **25** (2008), no. 4-5, 214–229.
[16] J. H. Kong, H. C. Lee, and G. I. Kim, *C^1 Hermite interpolation with PH curves by boundary data modification*, J. Comput. Appl. Math. **248** (2013), 47–60.
[17] J. H. Kong, S. Lee, and G. Kim, *Minkowski Pythagorean-hodograph preserving mappings*, J. Comput. Appl. Math. **308** (2016), 166–176.
[18] J. Kosinka and B. Jüttler, *C^1 Hermite interpolation by Pythagorean hodograph quintics in Minkowski space*, Adv. Comput. Math. **30** (2009), no. 2, 123–140.
[19] J. Kosinka and M. Lavicka, *A unified Pythagorean hodograph approach to the medial axis transform and offset approximation*, J. Comput. Appl. Math. **235** (2011), no. 12, 3413–3424.
[20] ———, *Pythagorean hodograph curves: a survey of recent advances*, J. Geom. Graph. **18** (2014), no. 1, 23–43.
[21] J. Kosinka and Z. Šìr, *C^2 Hermite interpolation by Minkowski Pythagorean hodograph curves and medial axis transform approximation*, Comput. Aided Geom. Design **27** (2010), no. 8, 631–643.
[22] S. Lee, H. C. Lee, M. R. Lee, S. Jeong, and G. I. Kim, *Hermite interpolation using Möbius transformations of planar Pythagorean-hodograph cubics*, Abstr. Appl. Anal. **2012** (2012), Art. ID 560246, 15 pp.
[23] H. P. Moon, *Minkowski Pythagorean hodographs*, Comput. Aided Geom. Design **16** (1999), no. 8, 739–753.
[24] F. Pelosi, R. T. Farouki, C. Manni, and A. Sestini, *Geometric Hermite interpolation by spatial Pythagorean-hodograph cubics*, Adv. Comput. Math. **22** (2005), no. 4, 325–352.
[25] Z. Šìr and B. Jüttler, *Euclidean and Minkowski Pythagorean hodograph curves over planar cubics*, Comput. Aided Geom. Design **22** (2005), no. 8, 753–770.

Gwangil Kim
Department of Mathematics and RINS
College of Natural Science
GyeongSang National University
Jinju 52828, Korea
Email address: gikim@gnu.ac.kr

Jae Hoon Kong
Department of Mathematics
GyeongSang National University
Jinju 52828, Korea
Email address: jhkong@gnu.ac.kr

Hyun Chol Lee
Department of Mathematics
GyeongSang National University
Jinju 52828, Korea
Email address: lhc5373@gnu.ac.kr